Original Manuscript

Journal of Vibration and Control
2022, Vol. 0(0) 1–12

DOI: 10.1177/10775463221138327
journals.sagepub.com/home/jvc
SAGE

Observer-based free-will arbitrary time sliding mode control for uncertain robotic manipulators

Huayang Sai[1,2], Zhenbang Xu[1], Tianyu Han[3], Xiaoming Wang[1], and Hang Li[1]

Abstract

This paper studies a free-will arbitrary time sliding mode control (FATSMC) based on the predefined-time sliding mode observer (PTSMO) for tracking control of robotic manipulators. First, a PTSMO is constructed to estimate the coupled uncertainty of the robotic manipulator system in a preset time. Then, a FATSMC scheme is proposed to realize the free-will arbitrary time tracking control for uncertain robotic manipulators and preset the upper bound on the settling time in the reaching phase. The proposed control strategy has high tracking accuracy and smooth control torque, while the convergence time of the system is nonconservative. The stability of the FATSMC and the PTSMO are rigorously demonstrated using the Lyapunov stability theory. Finally, a three-degree-of-freedom uncertain manipulator is utilized for numerical simulation. The effectiveness and superiority of the proposed control strategy are demonstrated by comparing it with several control strategies.

Keywords

free-will arbitrary stability, uncertain robotic manipulator, predefined-time sliding mode observer

1. Introduction

Tracking control of uncertain robotic manipulators has been paid much more attention in recent years, aiming to achieve higher tracking accuracy, fast response, and strong robustness. Among many control methods, the sliding mode control (SMC) technique has attracted much attention from scholars for its robustness, order reduction, ease of implementation, and design simplicity (Brahmi et al., 2020; Li et al., 2022). Up to now, the SMC has been used in a variety of applications for different control objectives, such as the chaotic systems and robotic manipulators (Ablay, 2009; Gambhire et al., 2021).

The purpose of the SMC is to force the tracking error to the sliding manifold and then converge to the origin along the sliding manifold (Drakunov and Utkin, 1992). Although the finite-time SMC (Hong et al., 2002) has received a great deal of research, its convergence time depends on the initial state of the system. For robotic manipulators, the initial states are not always available in advance, which means that the actual convergence time is hard to be guaranteed. To address this problem, a stronger property called the fixed-time stability was proposed, where the upper bound of the settling time is independent of the initial states (Polyakov, 2011). Some critical, theoretical, and mathematical analyses related to fixed-time stability were proposed in Polyakov et al. (2015); Zuo and Tie (2014, 2016), which facilitated the development and application of the fixed-time SMC. Benefiting from the fact that the convergence time of fixed-time SMC is independent of the initial state of the system, the fixed-time SMC has been extensively studied in the tracking control of robotic manipulators (Sai et al. 2021, 2022; Su et al., 2020; Zhang et al., 2019).

It is worth noting that although the upper bound on the settling time of the system is independent of the initial

[1]CAS Key Laboratory of On-orbit Manufacturing and Integration for Space Optics System, Changchun Institute of Optics, Fine Mechanics and Physics, Chinese Academy of Sciences, Changchun, China
[2]University of Chinese Academy of Sciences, Beijing, China
[3]School of Mechanical Engineering, Shanghai Jiao Tong University, Shanghai, China

Received: 13 April 2022; accepted: 21 October 2022

Corresponding author:
Zhenbang Xu, CAS Key Laboratory of On-orbit Manufacturing and Integration for Space Optics System, Changchun Institute of Optics, Fine Mechanics and Physics, Chinese Academy of Sciences, No. 3888 Dong Nanhu Road, Changchun 130033, China.
Email: xuzhenbang@ciomp.ac.cn

states, it is often challenging to find a direct relationship between the settling time and the system parameters, and in some cases, the settling time cannot be reduced to be less than a fixed-constant, even by tuning the system parameters. This motivates the formulation of prescribed-time and predefined-time stability (Sánchez-Torres et al., 2018b; Song et al., 2017). However, most of the predefined-time SMC schemes can only guarantee the predefined-time stability of the system in the reaching phase, and the actual convergence time is quite conservative compared to the preset settling time (Jiménez-Rodríguez et al., 2017b, 2018, 2020; Sánchez-Torres et al., 2015). As a response, a more advanced concept called free-will arbitrary time stabilization was proposed in Pal et al. (2020a). Subsequently, free-will arbitrary time control is combined with terminal sliding mode control (TSMC) to provide an overall settling time for the system and not only in the reaching phase (Pal et al., 2020b). However, the convergence time of the system in the reaching phase is finite-time stable and unknown, so it is necessary to determine the convergence time in the reaching phase by continuous iterations.

In addition to the problem mentioned above, the free-will arbitrary time controller in Pal et al., 2020b) is difficult to apply to tracking control of uncertain robotic manipulators because the upper bound of the coupled uncertainty of the robotic manipulator is often difficult to obtain. Meanwhile, overestimation of the upper bound on the system uncertainty leads to strong chattering of the controller. Fortunately, the observer is an effective tool to solve the above problems (Xiao et al., 2016; Xiao and Yin, 2018). In Chalanga et al. (2016); Rabiee et al. (2019), finite-time sliding mode disturbance observers were designed based on adaptive and super-twisting techniques, respectively. Additionally, in recent years, several fixed-time disturbance observers (Ni et al., 2017; Pan and Zhang, 2022; Zhang et al., 2019) have been proposed for estimating the external disturbances of the system in a fixed time. However, the above perturbation observers can only guarantee finite-time or fixed-time estimates of system perturbations, and few studies have addressed the design of predefined-time observer.

Driven by practical requirements for the uncertain robotic manipulators tracking control problem and inspired by previous discussions, a novel free-will arbitrary time sliding mode control (FATSMC) based on the predefined-time sliding mode observer (PTSMO) for uncertain robotic manipulators is investigated. To the best of the authors' knowledge, there is hardly any research on free-will arbitrary time controllers for tracking control of uncertain robotic manipulators. The contributions of this paper are twofold. First, a novel PTSMO is designed to enable estimation of the system coupled uncertainty in a preset amount of time. Unlike finite-time and fixed-time observers, the convergence time bounds of the designed observer are clearly given in the control design. Second, the reaching phase of the designed FATSMC is predefined-time stable, and the total settling time is free-will arbitrary time stable. Compared to the convergence time in the reaching phase obtained by constant updating in Pal et al. (2020b), the convergence time of the designed controller in the reaching phase can be pre-settable. Therefore, it avoids the excessive torques that result from achieving arbitrary time convergence by forcing the system state to converge rapidly to the origin in the sliding phase. Benefiting from the accurate estimation of the system coupled uncertainty, the designed control strategy avoids the overestimation of the upper bound of the external disturbance and thus reduces the system chattering.

The remainder of the paper is organized as follows. Some preliminaries and problem formulation are given in Section 2. In Section 3, we introduce the design of the controller and perform a stability analysis. Some numerical simulations and comparisons are given in Section 4, and the concluding remarks are summarized in Section 5.

Notation: In this paper, sgn(x) represents the signum function, and vector $\mathbf{sgn}(\boldsymbol{x}) \in \mathbb{R}^n$ is $\mathbf{sgn}(\boldsymbol{x}) = [\mathrm{sgn}(x_1), \ldots, \mathrm{sgn}(x_n)]^T$. The nonlinear function $\mathrm{sig}^\alpha(x)$ and vector $\mathbf{Sig}^\alpha(\boldsymbol{x}) \in \mathbb{R}^n$ represent $\mathrm{sig}^\alpha(x) = |x|^\alpha \mathrm{sgn}(x)$ and $\mathbf{Sig}^\alpha(\boldsymbol{x}) = [|x_1|^\alpha \mathrm{sgn}(x_1), \ldots, |x_n|^\alpha \mathrm{sgn}(x_n)]^T$, with $\alpha > 0$.

2. Preliminaries and problem formulation

2.1. Some definitions and lemmas

Considering an autonomous dynamical system

$$\dot{\boldsymbol{x}} = \boldsymbol{f}(\boldsymbol{x}, \boldsymbol{\rho}), \tag{1}$$

where $\mathbf{x} \in \mathbb{R}^n$ is the system state, and the vector $\boldsymbol{\rho} \in \mathbb{R}^n$ is the constant parameter of system (1). The nonlinear function $\boldsymbol{f} : \mathbb{R}^n \to \mathbb{R}^n$ satisfies $\boldsymbol{f}(0, \boldsymbol{\rho}) = 0$, and the initial state is $\boldsymbol{x}_0 = \boldsymbol{x}(0) \in \mathbb{R}^n$.

Definition 1. (Fixed-time stability) (Sánchez-Torres et al., 2018a) The origin of system (1) is globally fixed-time stable if it is globally finite-time stable (Bhat and Bernstein, 2000), and the settling time function $\mathrm{T} : \mathbb{R}^n \to \mathbb{R}_+ \cup \{0\}$ is bounded, that is, $\exists \mathrm{T}_{\max} > 0 : \forall x_0 \in \mathbb{R}^n : \mathrm{T}(x_0) \leqslant \mathrm{T}_{\max}$.

Definition 2. (Free-will arbitrary time stability) (Pal et al., 2020a) The origin of system (1) is free-will arbitrary time stable if it is fixed-time stable and there exists an arbitrary settling time $\mathrm{T}_f > 0 : \forall x_0 \in \mathbb{R}^n : \mathrm{T}(\boldsymbol{x}_0) \leqslant \mathrm{T}_f$.

Theorem 1. (Pal et al., 2020a) For system (1), if there is a bounded continuously differentiable function $V(x, t) : \mathbb{R}^n \times \mathbb{R}_+ \to \mathbb{R}^n, t \in [t_0, t_f]$ and a constant $\eta \geqslant 1$ such that

$$\begin{gathered} V(0, t) = 0, \forall t \geqslant t_0 \\ \dot{V} \leqslant -\frac{\eta(e^V - 1)}{e^V (t_f - t)}, \forall t \in [t_0, t_f), \end{gathered} \tag{2}$$

then the origin is free-will arbitrary time stable with an arbitrary settling time $T_f = t_f - t_0$.

Theorem 2. (Munoz-Vazquez et al., 2019) For system (1), if there exists a Lyapunov function $V(x)$ such that any solution $\boldsymbol{x}(t, \boldsymbol{x}_0)$ satisfies

$$\dot{V}(x) \leqslant -\frac{\pi}{\rho t_r}\left(V^{1-\rho/2} + V^{1+\rho/2}\right), \forall x \in \mathbb{R}^n \backslash \{0\}, \quad (3)$$

where $\rho \in (0, 1)$ is a defined parameter and $t_r > 0$ is a preset settling time. Then, the origin of system (1) is globally fixed-time stable with the settling time t_r.

Remark 1. A system satisfying Theorem 2 is also called predefined-time stable. The difference with free-will arbitrary time control is that the total time of stabilization of the predefined-time control cannot be guaranteed, but only the stability of the system during the sliding phase or the reaching phase. Meanwhile, the settling time bounds of free-will arbitrary time control are less conservative compared to the predefined-time control.

2.2 Dynamic model of uncertain robotic manipulators

Consider the dynamic equation of n degree-of-freedom (DOF) rigid robotic manipulators as

$$\boldsymbol{M}(\boldsymbol{q})\ddot{\boldsymbol{q}} + \boldsymbol{C}(\boldsymbol{q}, \dot{\boldsymbol{q}})\dot{\boldsymbol{q}} + \boldsymbol{G}(\boldsymbol{q}) = \boldsymbol{\tau} + \boldsymbol{\tau}_d, \quad (4)$$

where $\boldsymbol{q}, \dot{\boldsymbol{q}}, \ddot{\boldsymbol{q}} \in \mathbb{R}^n$ represent the joint position, velocity, and acceleration vector of the joint, respectively. Positive-definite matrix $\boldsymbol{M}(\boldsymbol{q})$, centripetal-Coriolis matrix $\boldsymbol{C}(\boldsymbol{q}, \dot{\boldsymbol{q}})$, and gravitational vector $\boldsymbol{G}(\boldsymbol{q})$ can be expressed as $\boldsymbol{M}(\boldsymbol{q}) = \boldsymbol{M}_0(\boldsymbol{q}) + \triangle\boldsymbol{M}(\boldsymbol{q}), \boldsymbol{C}(\boldsymbol{q}, \dot{\boldsymbol{q}}) = \boldsymbol{C}_0(\boldsymbol{q}, \dot{\boldsymbol{q}}) + \triangle\boldsymbol{C}(\boldsymbol{q}, \dot{\boldsymbol{q}})$, and $\boldsymbol{G}(\boldsymbol{q}) = \boldsymbol{G}_0(\boldsymbol{q}) + \triangle\boldsymbol{G}(\boldsymbol{q})$. $\boldsymbol{M}_0(\boldsymbol{q}), \boldsymbol{C}_0(\boldsymbol{q}, \dot{\boldsymbol{q}})$ and $\boldsymbol{G}_0(\boldsymbol{q})$ are the nominal parts of the model parameters, and $\triangle\boldsymbol{M}(\boldsymbol{q}), \triangle\boldsymbol{C}(\boldsymbol{q}, \dot{\boldsymbol{q}})$ and $\triangle\boldsymbol{G}(\boldsymbol{q})$ are the model uncertainties. $\boldsymbol{\tau}$ is the joint torque vector, and $\boldsymbol{\tau}_d$ represents the external disturbance. Then, system (4) can be written as

$$\ddot{\boldsymbol{q}} = -\boldsymbol{M}_0^{-1}(\boldsymbol{q})\left(\boldsymbol{C}_0\left(\boldsymbol{q}, \dot{\boldsymbol{q}}\right)\dot{\boldsymbol{q}} + \boldsymbol{G}_0(\boldsymbol{q})\right) + \boldsymbol{M}_0^{-1}(\boldsymbol{q})\boldsymbol{\tau} + \boldsymbol{D}_d \quad (5)$$

where $\boldsymbol{D}_d = \boldsymbol{M}_0^{-1}(\boldsymbol{q})(\boldsymbol{\tau}_d - \triangle\boldsymbol{M}(\boldsymbol{q})\ddot{\boldsymbol{q}} - \triangle\mathbf{C}(\boldsymbol{q}, \dot{\boldsymbol{q}})\dot{\boldsymbol{q}} - \Delta\boldsymbol{G}(\boldsymbol{q}))$ denotes the coupled uncertainty, and it consists of external disturbances and the effects on the system dynamics model due to errors in the system parameters.

Assumption 1. $\boldsymbol{D}_d$ is unknown but bounded and satisfies $|\dot{D}_{di}| \leqslant D_{1i}$.

Remark 2. The external disturbance of the robotic system consists mainly of frictional force, which is often bounded in the actual system. Therefore, it is reasonable to suppose the assumption that the coupled uncertainty of the system and its derivatives are bounded, and such assumption can be found in Jing et al. (2019).

3. Main results

In this section, a novel PTSMO and FATSMC are designed for uncertain robotic manipulator, respectively. Meanwhile, their stability is rigorously proved through the Lyapunov stability theory.

3.1. Design of PTSMO

Define the tracking error $\boldsymbol{e} = \boldsymbol{q} - \boldsymbol{q}_d$, where $\boldsymbol{q}_d$ represents the reference trajectory. For simplicity, three variables are introduced: $\boldsymbol{x}_1 = \boldsymbol{q}, \boldsymbol{x}_2 = \dot{\boldsymbol{q}}$, and $\boldsymbol{x}_3 = \boldsymbol{D}_d(\boldsymbol{x}_1, \boldsymbol{x}_2, \dot{\boldsymbol{x}}_2)$, where $\widehat{\boldsymbol{x}}_1, \widehat{\boldsymbol{x}}_2, \widehat{\boldsymbol{x}}_3$ represent the estimates of $\boldsymbol{x}_1$, $\boldsymbol{x}_2$, $\boldsymbol{x}_3$.

The PTSMO is designed as

$$\boldsymbol{\varepsilon} = \widehat{\boldsymbol{x}}_2 - \boldsymbol{x}_2 \quad (6)$$

$$\boldsymbol{\theta} = \dot{\boldsymbol{\varepsilon}} + \lambda_1 \mathbf{Sig}^{1-\rho}(\boldsymbol{\varepsilon}) + \lambda_2 \mathbf{Sig}^{1+\rho}(\boldsymbol{\varepsilon}) \quad (7)$$

$$\begin{aligned}\dot{\widehat{\boldsymbol{x}}}_2 = \; & \boldsymbol{M}_0^{-1}(\boldsymbol{x}_1)(\boldsymbol{\tau} - \boldsymbol{C}_0(\boldsymbol{x}_1, \boldsymbol{x}_2)\boldsymbol{x}_2 - \boldsymbol{G}_0(\boldsymbol{x}_1)) + \widehat{\boldsymbol{x}}_3 \\ & -\lambda_1 \mathbf{Sig}^{1-\rho}(\boldsymbol{\varepsilon}) - \lambda_2 \mathbf{Sig}^{1+\rho}(\boldsymbol{\varepsilon})\end{aligned} \quad (8)$$

$$\dot{\widehat{\boldsymbol{x}}}_3 = -\lambda_3 \mathbf{Sig}^{1-\rho}(\boldsymbol{\theta}) - \lambda_4 \mathbf{Sig}^{1+\rho}(\boldsymbol{\theta}) - \boldsymbol{\gamma}\mathbf{sgn}(\boldsymbol{\theta}) \quad (9)$$

where $\lambda_1 = 2^{\rho-2/2}\pi/\rho T_1$, $\lambda_2 = 2^{-\rho+2/2}\pi/\rho T_1$, $\lambda_3 = 2^{\rho-2/2}\pi/\rho T_2$, $\lambda_4 = 2^{-\rho+2/2}\pi/\rho T_2$, $\rho \in (0, 1)$ is a defined positive constant, and T_1, $T_2 > 0$ are two preset settling time parameters. $\boldsymbol{\gamma} = [\gamma_1, \ldots, \gamma_n]^T$ is a given vector satisfying $\gamma_i \geqslant D_{1i}$.

Theorem 3. Considering the uncertain robotic manipulator (4) with the bounded external disturbance, the estimated disturbance error and velocity error under the PTSMO (6)–(9) can converge to zero within T_2 and $T_1 + T_2$.

Proof. Taking the derivative of (6), we can have

$$\begin{aligned}\dot{\varepsilon} &= \dot{\widehat{\boldsymbol{x}}}_2 - \dot{\boldsymbol{x}}_2 \\ &= \widehat{\boldsymbol{x}}_3 - \boldsymbol{x}_3 - \lambda_1 \boldsymbol{Sig}^{1-\rho}(\varepsilon) - \lambda_2 \boldsymbol{Sig}^{1+\rho}(\varepsilon)\end{aligned} \quad (10)$$

Taking (10) into (7) yields $\boldsymbol{\theta} = \widehat{\boldsymbol{x}}_3 - \boldsymbol{x}_3$. Then, the derivative leads to

$$\begin{aligned}\dot{\boldsymbol{\theta}} &= \dot{\widehat{\boldsymbol{x}}}_3 - \dot{\boldsymbol{x}}_3 \\ &= -\lambda_3 \boldsymbol{Sig}^{1-\rho}(\varepsilon) - \lambda_4 \boldsymbol{Sig}^{1+\rho}(\varepsilon) - \boldsymbol{\gamma}\boldsymbol{sgn}(\boldsymbol{\theta}) - \dot{\boldsymbol{x}}_3.\end{aligned} \quad (11)$$

Choose the Lyapunov function as

$$V_1 = \frac{1}{2}\theta_i^2. \quad (12)$$

Then, from (11), it can be obtained

$$\begin{aligned}\dot{V}_1 &= \theta_i\dot{\theta}_i \\ &= \theta_i\left(-\lambda_3 \mathrm{sig}^{1-\rho}(\theta_i) - \lambda_4 \mathrm{sig}^{1+\rho}(\theta_i) - \gamma_i \mathrm{sgn}(\theta_i) - \dot{x}_{3i}\right) \\ &\leqslant -\lambda_3|\theta_i|^{2-\rho} - \lambda_4|\theta_i|^{2+\rho} - \left(\gamma_i - |\dot{x}_{3i}|\right)|\theta_i|.\end{aligned} \tag{13}$$

With Assumption 1, (13) can lead to

$$\begin{aligned}\dot{V}_1 &\leqslant -\lambda_3|\theta_i|^{2-\rho} - \lambda_4|\theta_i|^{2+\rho} \\ &= -2^{\frac{\rho-2}{2}}\frac{\pi}{\rho T_2}|\theta_i|^{2-\rho} - 2^{-\frac{\rho+2}{2}}\frac{\pi}{\rho T_2}|\theta_i|^{2+\rho} \\ &= -\frac{\pi}{\rho T_2}\left(V_1^{1-\rho/2} + V_1^{1+\rho/2}\right).\end{aligned} \tag{14}$$

According to Theorem 3, the inequality (14) satisfies the predefined-time stability, and the estimated coupled uncertainty error will converge to zero within the settling time T_2.

When the estimated coupled uncertainty converges to zero, such as $t \geqslant T_2$, (10) can lead to

$$\dot{\boldsymbol{\varepsilon}} = \dot{\hat{\boldsymbol{x}}}_2 - \dot{\boldsymbol{x}}_2 = -\lambda_1 \boldsymbol{Sig}^{1-\rho}(\boldsymbol{\varepsilon}) - \lambda_2 \boldsymbol{Sig}^{1+\rho}(\boldsymbol{\varepsilon}). \tag{15}$$

Choose the Lyapunov function

$$V_2 = \frac{1}{2}\varepsilon_i^2. \tag{16}$$

Taking the time derivative of (16), then we can have

$$\begin{aligned}\dot{V}_2 &= \varepsilon_i\dot{\varepsilon}_i = \varepsilon_i\left(-\lambda_1 \mathrm{sig}^{1-\rho}(\varepsilon_i) - \lambda_2 \mathrm{sig}^{1+\rho}(\varepsilon_i)\right) \\ &= -2^{\frac{\rho-2}{2}}\frac{\pi}{\rho T_1}|\varepsilon_i|^{2-\rho} - 2^{-\frac{\rho+2}{2}}\frac{\pi}{\rho T_1}|\varepsilon_i|^{2+\rho} \\ &= -\frac{\pi}{\rho T_1}\left(V_2^{1-\rho/2} + V_2^{1+\rho/2}\right).\end{aligned} \tag{17}$$

With Theorem 2, the estimated velocity error converges to zero within T_2 after the estimated coupled error converges to zero within. This completes the proof of Theorem 3.

3.2. Design of FATSMC based on PTSMO

Our objective is to design a novel FATSMC scheme based on the PTSMO in (6)–(9) to guarantee that the uncertain robotic manipulator achieves tracking of the reference trajectory within an arbitrary preset time. Our findings reveal that it can guarantee that the system state converges to the sliding mode surface (SMS) within a given t_r and then converges to the origin within a total preset time t_f ($t_f > t_r + T_1 + T_2$), as shown in Figure 1.

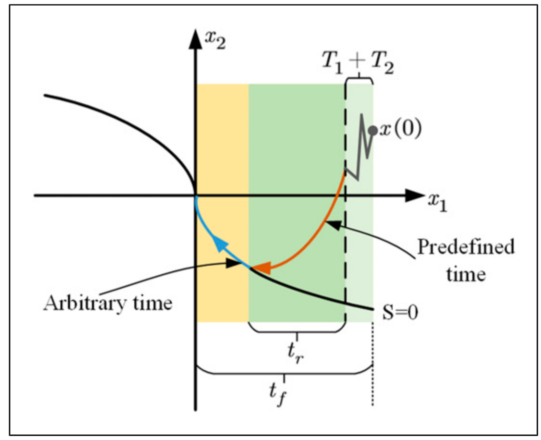

Figure 1. The phase plot of the system.

First, the SMS is designed as

$$\begin{cases} \boldsymbol{s} = \dot{\boldsymbol{e}} + w(\boldsymbol{e})\ 0 \leqslant t < t_f \\ \boldsymbol{s} = \kappa\boldsymbol{e} + \dot{\boldsymbol{e}}\ t \geqslant t_f \end{cases} \tag{18}$$

where κ is a defined positive constant, and $\dot{\boldsymbol{e}} = \boldsymbol{x}_2 - \dot{\boldsymbol{q}}_d$. t_f is an arbitrary given stability time constant. $w(\boldsymbol{e}) = [w(e_1), \ldots, w(e_i)]^T$ and $w(e_i)$ are nonlinear functions leading to free-will arbitrary time stabilization as

$$w(e_i) = \frac{\eta(1 - \exp(-e_i))}{t_f - t} \tag{19}$$

where i denotes the joint i, and $\eta > 1$ is a constant. It is easy to obtain the derivative of $w(e_i)$ with respect to time as

$$\dot{w}(e_i, \dot{e}_i) = \frac{\eta\left(\exp(e_i) - 1 + (t_f - t)\dot{e}_i\right)}{\exp(e_i)(t_f - t)^2} \tag{20}$$

Then, based on PTSMO (6)–(9) and SMS (18), the FATSMC scheme is constructed as (21)

In (21), $\varphi(\boldsymbol{s}) = [\varphi(s_1), \ldots, \varphi(s_n)]^T$ and $F(\boldsymbol{x}_1, \boldsymbol{x}_2)$ are expressed as

$$\begin{cases} \boldsymbol{\tau} = -\boldsymbol{M}_0(\boldsymbol{x}_1)\left[\varphi(\mathrm{s})\mathbf{sgn}(\boldsymbol{s}) + \dot{w}\left(\boldsymbol{e}, \dot{\boldsymbol{e}}\right) - \lambda_1 \mathbf{Sig}^{1-\rho}(\varepsilon_1) - \lambda_2 \mathbf{Sig}^{1+\rho}(\varepsilon_1) + F(\boldsymbol{x}_1, \boldsymbol{x}_2) + \hat{\boldsymbol{x}}_3\right],\ 0 \leqslant t < t_f \\ \boldsymbol{\tau} = -\boldsymbol{M}_0(\boldsymbol{x}_1)\left[\kappa\hat{\boldsymbol{e}} + \hat{\boldsymbol{x}}_3 + F(\boldsymbol{x}_1, \boldsymbol{x}_2) - \lambda_1 \mathbf{Sig}^{1-\rho}(\varepsilon_1) - \lambda_2 \mathbf{Sig}^{1+\rho}(\varepsilon_1)\right],\ t \geqslant t_f \end{cases} \tag{21}$$

$$\varphi(s_i) = \frac{\pi}{\rho t_r}\left(|s_i|^{1-\frac{\rho}{2}} + |s_i|^{1+\frac{\rho}{2}}\right) \tag{22}$$

$$F(\boldsymbol{x}_1,\boldsymbol{x}_2) = -\boldsymbol{M}_0^{-1}(\boldsymbol{x}_1)(\boldsymbol{C}_0(\boldsymbol{x}_1,\boldsymbol{x}_2)\boldsymbol{x}_2 + \boldsymbol{G}_0(\boldsymbol{x}_1)) - \ddot{\boldsymbol{q}}_d \tag{23}$$

where t_r and ρ are two defined positive constants satisfying $T_1 + T_2 + t_r < t_f$ and $0 < \rho < 1$.

The flowchart diagram of the FATSMC based on the PTSMO is presented in Figure 2.

Remark 3. In practical model-based dynamics control applications of robotic manipulators, the main limitations on control performance are (i) knowledge of the upper bound of the robotic system model or dynamical system, (ii) system uncertainty and external disturbances, and (iii) the feasibility of control inputs (Boukattaya et al., 2018). For the proposed control strategy, neither accurate dynamics nor a priori knowledge of the upper bound of disturbances is required. Moreover, in general, the position and velocity of the robotic joints can be generally obtained by encoders or tachometers. Therefore, the proposed control strategy can be applied to the actual robotic control and does not suffer from harmful chattering. Modeling the dynamics of a multi-DOF robotic manipulator may be an essential challenge, but techniques such as neural networks may provide an effective way to address this problem.

Theorem 4. With PTSMO (6)–(9), the uncertain robotic manipulator system (4) attains predefined-time stability in the reaching phase within $t_r + T_1 + T_2$ and free-will arbitrary time stability within t_f if the SMS is selected as (18), and the control strategy is designed in (21)–(23).

Proof. First, considering $0 \leqslant t < t_f$, the stability discussion of the proposed control strategy is divided into the reaching phase and the sliding phase.

In the reaching phase, taking the time derivative of SMS (18), it can obtain that

$$\dot{\boldsymbol{s}} = \ddot{\boldsymbol{e}} + \dot{w}(\boldsymbol{e},\dot{\boldsymbol{e}}) = \dot{\boldsymbol{x}}_2 - \ddot{\boldsymbol{q}}_d + \dot{w}(\boldsymbol{e},\dot{\boldsymbol{e}}) \tag{24}$$

When $t > T_1 + T_2$, it has $x_2 = \hat{x}_2$. Then, combining with PTSMO (8), (24) can lead to

$$\begin{aligned}\dot{\boldsymbol{s}} &= \hat{\boldsymbol{x}}_3 - \lambda_1\mathbf{Sig}^{1-\rho}(\boldsymbol{\varepsilon}_1) - \lambda_2\mathbf{Sig}^{1+\rho}(\boldsymbol{\varepsilon}_1) \\ &\quad + \boldsymbol{M}_0^{-1}(\boldsymbol{x}_1)(\boldsymbol{\tau} - \boldsymbol{C}_0(\boldsymbol{x}_1,\boldsymbol{x}_2)\boldsymbol{x}_2 - \boldsymbol{G}_0(\boldsymbol{x}_1)) - \ddot{\boldsymbol{q}}_d + \dot{w}(\boldsymbol{e},\dot{\boldsymbol{e}}) \\ &= \hat{\boldsymbol{x}}_3 - \lambda_1\mathbf{Sig}^{1-\rho}(\boldsymbol{\varepsilon}_1) - \lambda_2\mathbf{Sig}^{1+\rho}(\boldsymbol{\varepsilon}_1) + \boldsymbol{M}_0^{-1}(\boldsymbol{x}_1)\boldsymbol{\tau} \\ &\quad + \dot{w}(\boldsymbol{e},\dot{\boldsymbol{e}}) + F(\boldsymbol{x}_1,\boldsymbol{x}_2).\end{aligned} \tag{25}$$

Taking the control torque (21) into (25) derives to

$$\dot{\boldsymbol{s}} = -\varphi(\boldsymbol{s})\mathbf{sgn}(\boldsymbol{s}). \tag{26}$$

For any joint i, consider the candidate Lyapunov function as $V_3 = |s_i|$. Then, it has

$$\begin{aligned}\dot{V}_3 &= -\dot{s}_i\mathrm{sgn}(s_i) = -\frac{\pi}{\rho t_r}\left(|s_i|^{1-\frac{\rho}{2}} + |s_i|^{1+\frac{\rho}{2}}\right) \\ &= -\frac{\pi}{\rho t_r}\left(V_3^{1-\frac{\rho}{2}} + V_3^{1+\frac{\rho}{2}}\right).\end{aligned} \tag{27}$$

According to Theorem 2, it can draw that the SMS can be reached within the preset time $t_r + T_1 + T_2$.

Once the system tracking error is constrained to the manifold $s_i = 0$, the following reduced-order dynamics can be obtained from (18) as

$$\dot{e}_i = -w(e_i) = -\frac{\eta(1 - exp(-e_i))}{t_f - t}. \tag{28}$$

According to Theorem 1, the position error e_i and the velocity error $\dot{e}_i$ can converge to zero within the arbitrary time t_f.

Then, considering the stability analysis for $t \geqslant t_f$, the SMC is switched to the linear surface $\boldsymbol{s} = \kappa\boldsymbol{e} + \dot{\boldsymbol{e}}$. With the PTSMO in (8), the derivative of $\boldsymbol{s}$ can be obtained as

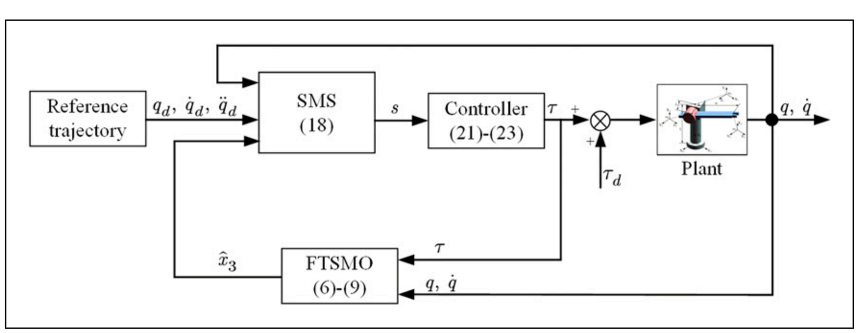

Figure 2. Block diagram of the proposed FATSMC based on the PTSMO.

$$\dot{s} = \kappa\dot{e} + \ddot{e} = \kappa\dot{e} + \widehat{x}_3 - \lambda_1\mathbf{Sig}^{1-\rho}(\varepsilon) - \lambda_2\mathbf{Sig}^{1+\rho}(\varepsilon) - \ddot{q}_d + M_0^{-1}(x_1)(\tau - C_0(x_1,x_2)x_2 - G_0(x_1)) = \kappa e + \widehat{x}_3 + M_0^{-1}(x_1)\tau - \lambda_1\mathbf{Sig}^{1-\rho}(\varepsilon) - \lambda_2\mathbf{Sig}^{1+\rho}(\varepsilon) + F(x_1,x_2) \tag{29}$$

Taking the control torque τ in (21) when $t \geqslant t_f$ into (29), it has $\dot{s} = 0$. Therefore, with the control torque, the position error e_i and the velocity error $\dot{e}_i$ can maintain their acquired equilibrium position for $t \geqslant t_f$, regardless of the external disturbance and the model uncertainties. This completes our proof.

Remark 4. Different from the free-will arbitrary time control strategy in Pal et al. (2020b), the reaching time in the proposed controller is explicit and independent of the initial state of the system. Therefore, reasonable t_r and t_f can be preset to avoid the high control requirements when the convergence time is close to t_f.

Remark 5. Unlike the most existing predefined-time controllers (Jiménez-Rodríguez et al., 2017a, 2017b, 2019; Sánchez-Torres et al., 2018a), the actual convergence time of the proposed control strategy is more nonconservative compared to the preset convergence time, which facilitates the selection of a more reasonable settling-time parameter.

Remark 6. Besides the preset time parameters, only control parameters η, ρ, κ, and γ should be chosen. Compared with the fixed-time controllers (Sai et al., 2021; Su et al., 2020; Zhang et al., 2019) and predefined-time controllers (Jiménez-Rodríguez et al., 2020; Krishnamurthy et al., 2021), fewer tuning parameters facilitate the practical application of the control strategy.

Remark 7. The control parameters ρ in FATSMC can be different from that in PTSMO, but they are generally chosen to be 0.5 to simplify the control strategy. The settling time T_1 and T_2 should be chosen as small as possible to ensure that the observer is able to estimate the coupled uncertainty of the system quickly. However, too small T_1 and T_2 can lead to drastic changes in the value of the observer during the initial phase, which can affect the control performance of the controller. Similarly, a smaller t_f means that the tracking error of the system can converge faster, but leads to an increase in the control torque and therefore requires a trade-off between the control performance and the control input.

Remark 8. According to (5), the proposed control scheme can be easily extended to a class of general dual integrator systems with the form of

$$\begin{cases} \dot{x}_1 = x_2 \\ \dot{x}_2 = f(x_1,x_2) + B(x_1,x_2)\tau + \Delta(t,x_1,x_2) \end{cases} \tag{30}$$

where $x_1, x_2 \in \mathbb{R}^n$, $f(x_1,x_2)$, and $g(x_1,x_2)$ are two vector functions, and $\Delta(t,x_1,x_2)$ is the uncertain term. Therefore, the designed controller can be applied to the control of mechanical systems such as inverted pendulums and permanent magnet linear motors.

4. Simulation and comparison

In this section, three numerical simulation examples are shown to illustrate the effectiveness and superiority of the proposed control strategy. The numerical simulations are programmed in Simulink of MATLAB R2020a, based on the Euler integrator and 10^{-3} fundamental sample time.

As shown in Figure 3, a 3-DOF robotic manipulator (He et al., 2017) is considered. The robotic manipulator includes two rotary joints and a prismatic joint, and the two rotation angles of rotary joints are defined as q_1 and q_2, and the translational of the prismatic joint is defined as q_3. The dynamics model of the robotic manipulator can be represented as

$$M(q) = \begin{bmatrix} M_{11} & M_{12} & M_{13} \\ M_{21} & M_{22} & 0 \\ M_{31} & 0 & M_{33} \end{bmatrix} \tag{31}$$

$$C(q,\dot{q}) = \begin{bmatrix} C_{11} & C_{12} & C_{13} \\ C_{21} & C_{22} & C_{23} \\ C_{31} & C_{32} & 0 \end{bmatrix} \tag{32}$$

$$G(q) = \begin{bmatrix} 0 \\ G_{21} \\ G_{31} \end{bmatrix} \tag{33}$$

where
$M_{11} = m_3q_3^2 sinq_2^2 + m_3l_1^2 + m_2l_1^2 + (1/4)m_1l_1^2, M_{12} = M_{21} = m_3q_3l_1cosq_2$, $M_{13} = M_{31} = m_3l_1sinq_2$, $M_{22} = m_3q_3^2 + (1/4) m_2l_2^2$, $M_{33} = m_3$, $C_{11} = m_3q_3^2sinq_2cosq_2\dot{q}_2 + m_3q_3^2sinq_2^2\dot{q}_3$, $C_{12} = m_3q_3^2sinq_2cosq_2\dot{q}_1 - m_3l_1q_3sinq_2\dot{q}_2 - m_3l_1q_3sinq_2\dot{q}_3$,

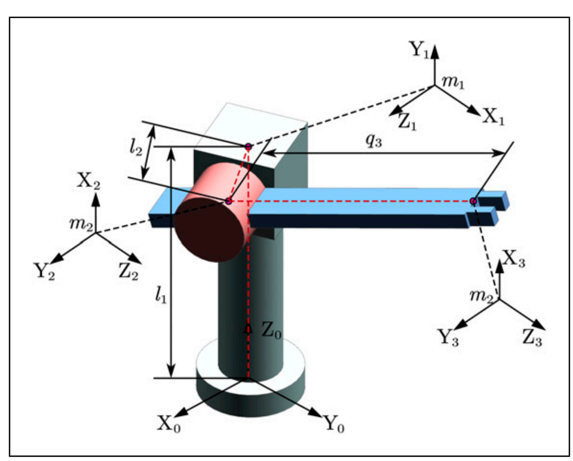

Figure 3. Coordinate frame for each link utilizing D-H method.

$C_{13} = m_3 q_3^2\ sinq_2^2 \dot{q}_1 -\ m_3 l_1 q_3\ sinq_2 \dot{q}_2$, $C_{21} = -m_3 q_3 sinq_2\ cosq_2 \dot{q}_1$, $C_{22} = m_3 q_3 \dot{q}_3$, $C_{23} = m_3 q_3 \dot{q}_2 + m_3 l_1 cosq_2 \dot{q}_3$, $C_{31} = -m_3 q_3 sinq_2^2 \dot{q}_1 + m_3 l_1 cosq_2 \dot{q}_2$, $C_{32} = m_3 l_1 cosq_2 \dot{q}_1 - m_3 q_3 \dot{q}_2, G_{21} = -m_3 g q_3 cosq_2, G_{31} = -m_3 g sinq_2$. Nominal model parameters of the manipulator are chosen as l_{10}= 0.3 m, l_{20}= 0.4 m, m_{10}= 2 kg, m_{20}= 2 kg, and m_{30}= 1 kg, and the actual model parameters are l_1= 0.3 m, l_2= 0.4 m, m_1= 2 kg, m_2= 2.1 kg, and m_3= 1.1 kg, and m_i

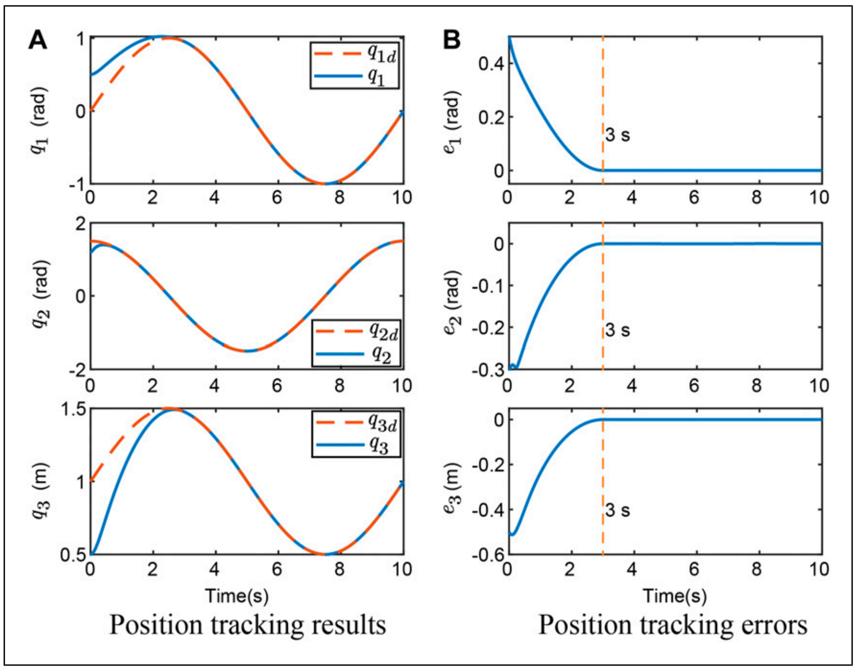

Figure 4. Position tracking results and errors.

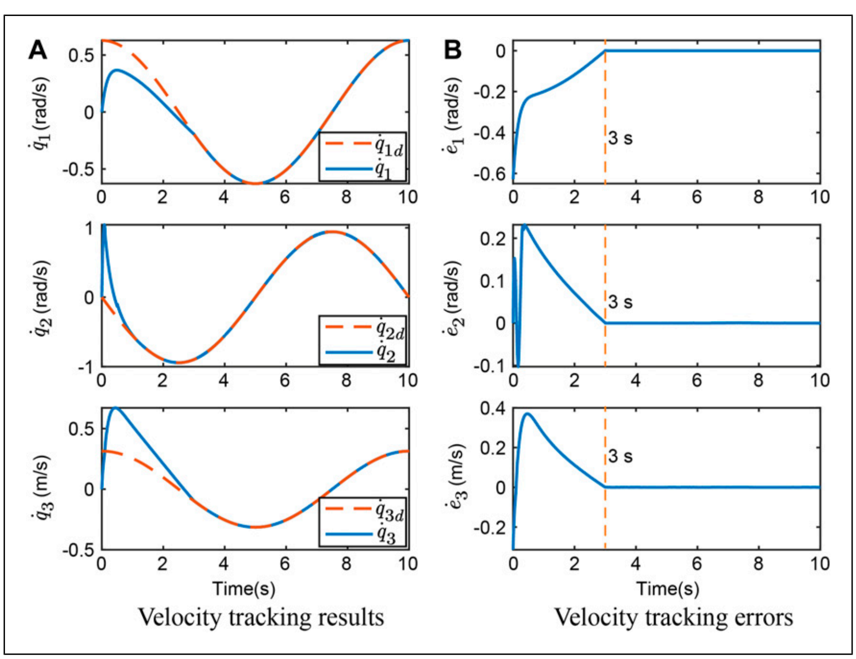

Figure 5. Velocity tracking results and errors.

denotes the equivalent lumped masses of links i. The external disturbance $\boldsymbol{\tau}_d$ is chosen as $\boldsymbol{\tau}_d = [sin(t)+1, 2cos(t) + 0.5, 2\ sin(t) + 1]^T$.

Example 1. The control goal is to make the output $\boldsymbol{q}$ track the target trajectory $\boldsymbol{q}_d = [sin(0.2\pi t), 1.5cos(0.2\pi t), 1 + 0.5sin(0.2\pi t)]^T$. The initial states are set as $\boldsymbol{q}(0) = [0.5, 1.2, 0.5]^T$ and $\dot{\boldsymbol{q}}(0) = [0, 0, 0]^T$. The control parameters in the PTSMO are chosen as $\boldsymbol{\gamma} = [20\ 20\ 20]^T$, $\rho = 0.5$, $T_1 = T_2 = 0.5$, and the initial estimate is set as $\hat{\boldsymbol{x}}_2 = \hat{\boldsymbol{x}}_3 = [0\ \ 0\ \ 0]^T$. The other control parameters in the FATSMC are set as $\eta = 2$, $\kappa = 5$, $t_r = 1.5$ and $t_f = 3$.

Simulation results are shown in Figures 4–7. From Figures 4 and 5, it can be seen that the position errors and velocity errors can converge to zero when $t = 3\ s$, which is consistent with the given settling time t_f. Figure 6 shows that the proposed control strategy can guarantee the smooth control torque. Figure 7 shows that FATSMC based on the PTSMO can accurately estimate the velocity and coupled uncertainty of each joint accurately within the predefined time. This example illustrates the effectiveness of the proposed controller through different performance metrics.

Example 2. To further illustrate the free-will arbitrary time stability of the proposed controller, four different initial states are considered as Case 1: $\boldsymbol{q}(0) = [0.7\ 1.1\ 0.4]^T$; Case 2: $\boldsymbol{q}(0) = [0.2\ 1.4\ 0.8]^T$; Case 3: $\boldsymbol{q}(0) = [-0.2\ 1.6\ 1.2]^T$; and Case 4: $\boldsymbol{q}(0) = [-0.7\ 1.8\ 1.4]^T$. The desired trajectory and control parameters are the same as Example 1.

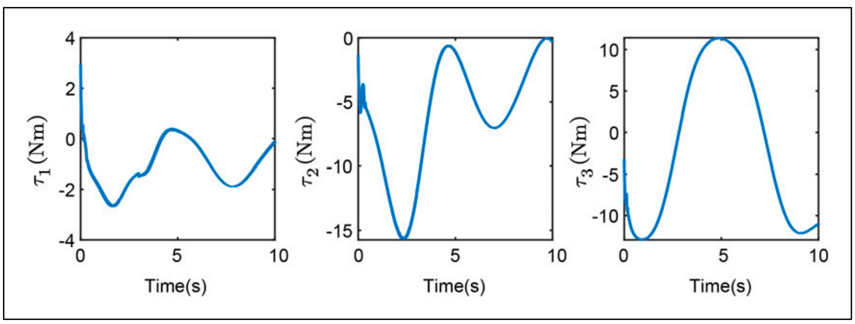

Figure 6. Control torque.

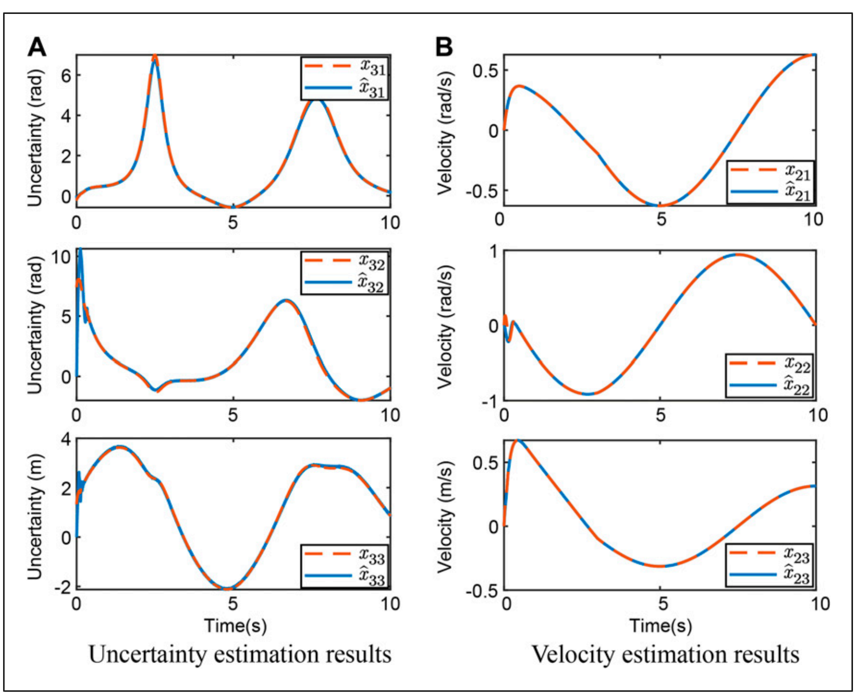

Figure 7. Uncertainty and velocity estimation results.

The simulation results are shown in Figure 8. It can be seen that the tracking errors can always converge to zero at $t_f = 3$ s without changing with different initial states. Therefore, for operational tasks with strict time requirements, the initial state of the system is not required, and arbitrary time convergence of the robotic system can be achieved by choosing the parameter t_f.

Example 3. To further demonstrate the advantages of the proposed control scheme, several existing SMC schemes with different stability are utilized to compare with the proposed control scheme, including the nonsingular fast terminal SMC (NFTSMC) (Yang and Yang, 2011), the fixed-time terminal SMC (Fixed TSMC) (Zhang et al., 2019), and the second-order predefined-time SMC (SOPSMC) (Jiménez-Rodríguez et al., 2017a). For a fair comparison, the settling time in the SOPSMC was set to 3 s, and the boundary layer approach was not considered in all controllers. The initial state and the desired trajectory are used in Example 1.

The simulation results are shown in Figures 9 and 10, and we can obtain that the proposed control strategy can

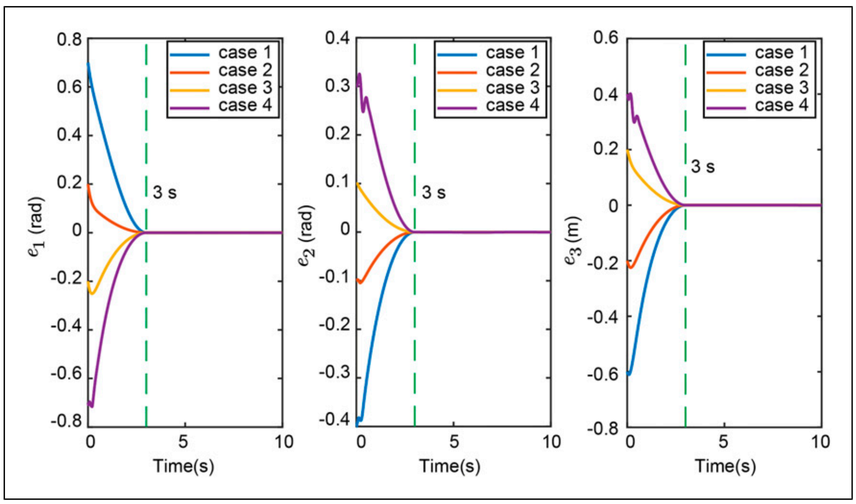

Figure 8. Position tracking results with different initial states.

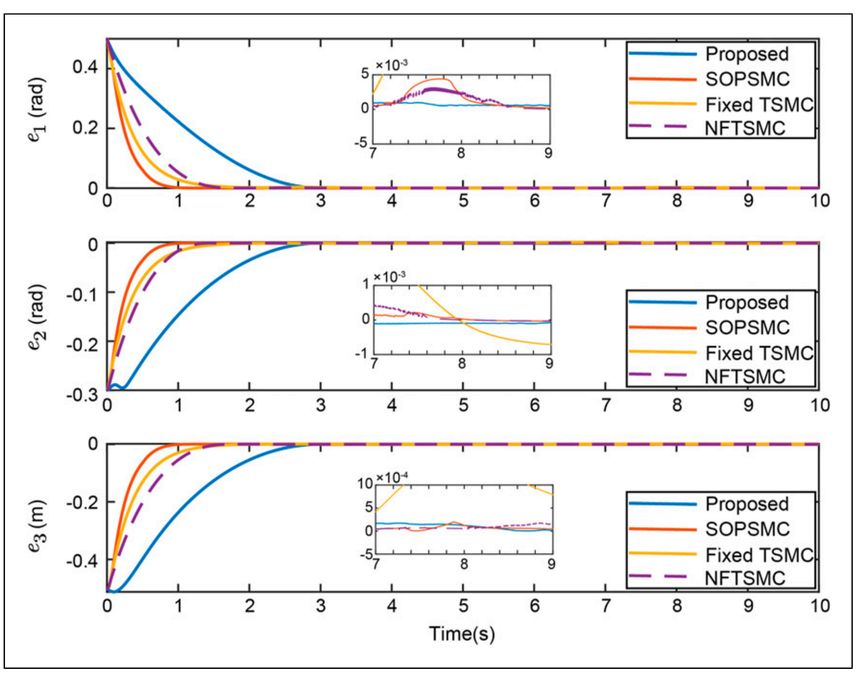

Figure 9. Comparison on tracking errors.

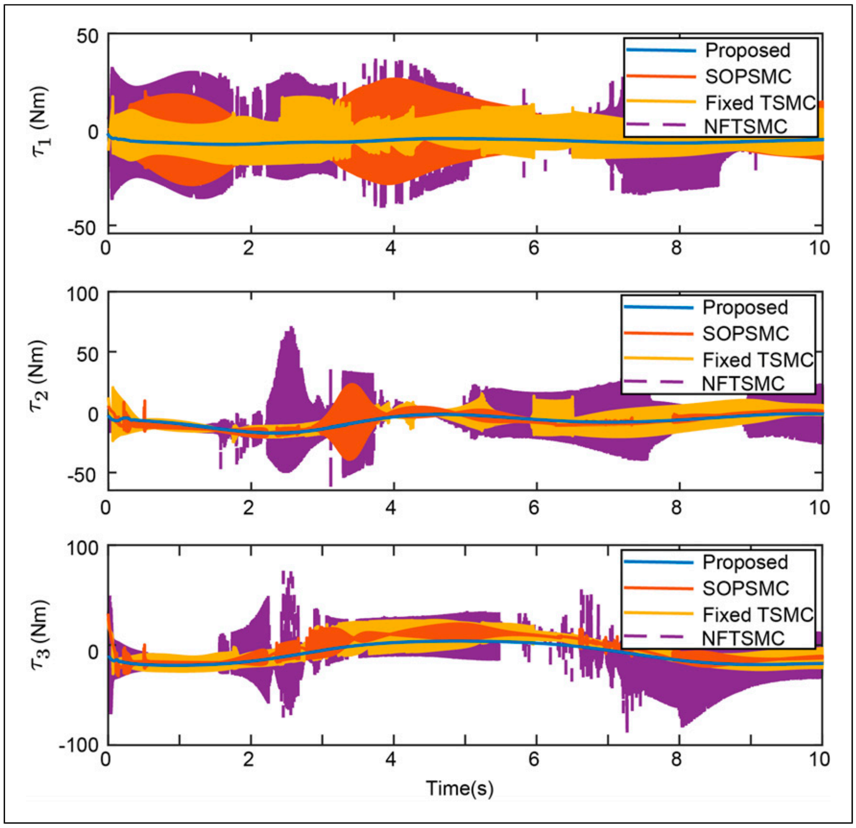

Figure 10. Comparison on control torque.

obtain higher position tracking accuracy and significantly smoother control torque. As a predefined-time controller, the actual convergence time of SOPSMC is quite conservative as mentioned in Remark 4, compared to the preset settling time of 3 s. For the three existing control schemes, the signum function is used to suppress the disturbances. However, the discontinuity of the signum function leads to strong chattering.

Moreover, as a finite-time stabilization controller, the actual convergence time of NFTSMC depends on the initial state of the system. For fixed-time controllers, there is a complex tuning relationship between the convergence time of Fixed TSMC and the control parameters. For most of the predefined-time controllers, such as SOPSMC, their stability time bounds tend to be very conservative, which leads to undesired convergence rates. The overall settling time of the proposed controller depends on only one control parameter, and the settling time bound is quite nonconservative. Besides, with the designed PTSMO, the priori knowledge of the upper bound of the coupled uncertainty is not necessary, and the chattering of the controller is avoided.

5. Conclusion

In this work, a FATSMC scheme based on the PTSMO has been presented for uncertain robotic manipulators. A novel PTSMO and FATSMC strategy are designed to guarantee free-will arbitrary time stability and the predefined-time convergence in the reaching phase for manipulators, which means that the total settling time of the system and the settling time in the reaching phase are available in advance. Additionally, the proposed PTSMO guarantees that the estimation of the coupled uncertainty of the system can be completed in a predetermined time and avoids a priori knowledge of the upper bound of the coupled uncertainty. Compared with existing SMC schemes, numerical simulation results show that the designed controller has higher tracking accuracy and less chattering while ensuring a less conservative actual convergence time with significant economic benefits. Some future work will mainly focus on the experimental evaluation of our approach by actual robotic manipulator systems to verify the availability of the proposed control scheme.

Declaration of conflicting interests

The author(s) declared no potential conflicts of interest with respect to the research, authorship, and/or publication of this article.

Funding

The author(s) disclosed receipt of the following financial support for the research, authorship, and/or publication of this article: This work was supported by the National Natural Science Foundation of China Under Grant No. 11972343 and Jilin Province Science and Technology Research Project Under Grant No. 20200404149YY.

ORCID iDs

Zhenbang Xu https://orcid.org/0000-0002-4120-2448
Tianyu Han https://orcid.org/0000-0002-6837-4901

References

Ablay G (2009) Sliding mode control of uncertain unified chaotic systems. *Nonlinear Analysis: Hybrid Systems* 3(4): 531–535.

Bhat SP and Bernstein DS (2000) Finite-time stability of continuous autonomous systems. *SIAM Journal on Control and Optimization* 38(3): 751–766.

Boukattaya M, Mezghani N and Damak T (2018) Adaptive nonsingular fast terminal sliding-mode control for the tracking problem of uncertain dynamical systems. *ISA Transactions* 77: 1–19.

Brahmi B, Laraki MH, Brahmi A, et al. (2020) Improvement of sliding mode controller by using a new adaptive reaching law: theory and experiment. *ISA Transactions* 97: 261–268.

Chalanga A, Kamal S, Fridman LM, et al. (2016) Implementation of super-twisting control: super-twisting and higher order sliding-mode observer-based approaches. *IEEE Transactions on Industrial Electronics* 63(6): 3677–3685.

Drakunov SV and Utkin VI (1992) Sliding mode control in dynamic systems. *International Journal of Control* 55(4): 1029–1037.

Gambhire S, Kishore DR, Londhe P, et al. (2021) Review of sliding mode based control techniques for control system applications. *International Journal of Dynamics and Control* 9(1): 363–378.

He W, Huang H and Ge SS (2017) Adaptive neural network control of a robotic manipulator with time-varying output constraints. *IEEE Transactions on Cybernetics* 47(10): 3136–3147.

Hong Y, Xu Y and Huang J (2002) Finite-time control for robot manipulators. *Systems & Control Letters* 46(4): 243–253.

Jiménez-Rodríguez E, Loukianov AG and Sánchez-Torres JD (2017a) A second order predefined-time control algorithm. In: 2017 14th International Conference on Electrical Engineering, Computing Science and Automatic Control (CCE), Mexico City, Mexico, 20–22 October 2017. pp. 1–6.

Jiménez-Rodríguez E, Muñoz-Vázquez AJ, Sánchez-Torres JD, et al. (2020) A lyapunov-like characterization of predefined-time stability. *IEEE Transactions on Automatic Control* 65(11): 4922–4927.

Jiménez-Rodríguez E, Muñoz-Vázquez AJ, Sánchez-Torres JD, et al. (2018) A note on predefined-time stability. *IFAC-PapersOnLine* 51(13): 520–525.

Jiménez-Rodríguez E, Sánchez-Torres JD, Gómez-Gutiérrez D, et al. (2019) Variable structure predefined-time stabilization of second-order systems. *Asian Journal of Control* 21(3): 1179–1188.

Jiménez-Rodríguez E, Sánchez-Torres JD and Loukianov AG (2017b) On optimal predefined-time stabilization. *International Journal of Robust and Nonlinear Control* 27(17): 3620–3642.

Jing C, Xu H and Niu X (2019) Adaptive sliding mode disturbance rejection control with prescribed performance for robotic manipulators. *ISA Transactions* 91: 41–51.

Krishnamurthy P, Khorrami F and Krstic M (2021) Adaptive output-feedback stabilization in prescribed time for nonlinear systems with unknown parameters coupled with unmeasured states. *International Journal of Adaptive Control and Signal Processing* 35(2): 184–202.

Li Y, Sai H, Zhu M, et al. (2022) Neural network-based continuous finite-time tracking control for uncertain robotic systems with actuator saturation. *Asian Journal of Control*. in press.

Munoz-Vazquez AJ, Sánchez-Torres JD, Jimenez-Rodriguez E, et al. (2019) Predefined-time robust stabilization of robotic manipulators. *IEEE* 24(3): 1033–1040.

Ni J, Liu L, Chen M, et al. (2017) Fixed-time disturbance observer design for brunovsky systems. *IEEE Transactions on Circuits and Systems II: Express Briefs* 65(3): 341–345.

Pal AK, Kamal S, Nagar SK, et al. (2020a) Design of controllers with arbitrary convergence time. *Automatica* 112: 108710.

Pal AK, Kamal S, Yu X, et al. (2020b) Free-will arbitrary time terminal sliding mode control. *IEEE Transactions on Circuits and Systems II: Express Briefs* DOI: 10.1109/TCSII.2020.3028175.

Pan H and Zhang G (2022) Observer-based fixed-time control for nonlinear systems with enhanced nonsingular fast terminal sliding mode. *Journal of Vibration and Control*: 10775463211053914. in press.

Polyakov A (2011) Nonlinear feedback design for fixed-time stabilization of linear control systems. *IEEE Transactions on Automatic Control* 57(8): 2106–2110.

Polyakov A, Efimov D and Perruquetti W (2015) Finite-time and fixed-time stabilization: implicit lyapunov function approach. *Automatica* 51: 332–340.

Rabiee H, Ataei M and Ekramian M (2019) Continuous nonsingular terminal sliding mode control based on adaptive sliding mode disturbance observer for uncertain nonlinear systems. *Automatica* 109: 108515.

Sai H, Xu Z, He S, et al. (2021) Adaptive nonsingular fixed-time sliding mode control for uncertain robotic manipulators under actuator saturation. *ISA Transactions* 123: 46–60.

Sai H, Xu Z, Xia C, et al. (2022) Approximate continuous fixed-time terminal sliding mode control with prescribed performance for uncertain robotic manipulators. *Nonlinear Dynamics* 110(1): 431–448.

Sánchez-Torres JD, Defoort M and Muñoz-Vázquez AJ (2018a) A second order sliding mode controller with predefined-time convergence. In: 2018 15th International conference on electrical engineering, computing science and automatic control (CCE), Mexico City, Mexico, 05–07 September 2018, pp. 1–4.

Sánchez-Torres JD, Gómez-Gutiérrez D, López E, et al. (2018b) A class of predefined-time stable dynamical systems. *IMA Journal of Mathematical Control and Information* 35(-Supplement_1): i1–i29.

Sánchez-Torres JD, Sanchez EN and Loukianov AG (2015) Predefined-time stability of dynamical systems with sliding modes. In: 2015 American control conference (ACC), Chicago, IL, USA, 01–03 July 2015, pp. 5842–5846.

Song Y, Wang Y, Holloway J, et al. (2017) Time-varying feedback for regulation of normal-form nonlinear systems in prescribed finite time. *Automatica* 83: 243–251.

Su Y, Zheng C and Mercorelli P (2020) Robust approximate fixed-time tracking control for uncertain robot manipulators. *Mechanical Systems and Signal Processing* 135: 106379.

Xiao B and Yin S (2018) Exponential tracking control of robotic manipulators with uncertain dynamics and kinematics. *IEEE Transactions on Industrial Informatics* 15(2): 689–698.

Xiao B, Yin S and Kaynak O (2016) Tracking control of robotic manipulators with uncertain kinematics and dynamics. *IEEE Transactions on Industrial Electronics* 63(10): 6439–6449.

Yang L and Yang J (2011) Nonsingular fast terminal sliding-mode control for nonlinear dynamical systems. *International Journal of Robust and Nonlinear Control* 21(16): 1865–1879.

Zhang L, Wang Y, Hou Y, et al. (2019) Fixed-time sliding mode control for uncertain robot manipulators. *IEEE Access* 7: 149750–149763.

Zuo Z and Tie L (2014) A new class of finite-time nonlinear consensus protocols for multi-agent systems. *International Journal of Control* 87(2): 363–370.

Zuo Z and Tie L (2016) Distributed robust finite-time nonlinear consensus protocols for multi-agent systems. *International Journal of Systems Science* 47(6): 1366–1375.